



Enhanced photocatalytic activity for degrading Rhodamine B solution of commercial Degussa P25 TiO₂ and its mechanisms

Xu Qin^a, Liqiang Jing^{a,b,*}, Guohui Tian^a, Yichun Qu^a, Yujie Feng^{b,**}

^a Key Laboratory of Functional Inorganic Materials Chemistry, Heilongjiang University, Ministry of Education, School of Chemistry and Materials Science, Harbin 150080, PR China

^b State Key Lab of Urban Water Resource and Environment, Harbin Institute of Technology, Harbin 150001, PR China

ARTICLE INFO

Article history:

Received 23 April 2009

Received in revised form 28 July 2009

Accepted 28 July 2009

Available online 4 August 2009

Keywords:

Degussa P25 TiO₂

Surface-modification

Anatase thermal stability

Photoinduced charge separation

Photocatalysis

ABSTRACT

In this paper, the Degussa P25 TiO₂ (P-TiO₂) is modified by the post-treatment with the phosphorous acid, and the resulting samples are also characterized by X-ray Powder Diffraction (XRD), Raman spectra (Raman), Brunauer–Emmett–Teller (BET) surface area analyzer, Transmission Electron Microscopy (TEM), Fourier Transform Infrared Spectra (FT-IR), X-ray Photoelectron Spectroscopy (XPS), Ultraviolet–Visible Diffuse Reflectance Spectra (UV–vis DRS) and Surface Photovoltage Spectroscopy (SPS). The effects of surface-modification on the thermal stability and photocatalytic activity of the P-TiO₂ are investigated in detail. The results show that the surface-modification enhances the thermal stability of P-TiO₂, even still with a main anatase phase after thermal treatment at 900 °C, which is close related to the inhibition effects of the PO₄³⁻ groups on the surface mass diffusion as well as the directing connections of P-TiO₂ nanoparticles. Interestingly, the modified P-TiO₂ by thermal treatment at 700 and 800 °C can exhibit much higher photocatalytic activity than un-modified ones. The reasons for the activity enhancement are involved with the enhanced anatase thermal stability, consequently improving photoinduced charge separation rate, and still keeping large surface area and a certain amount of surface hydroxyl groups.

© 2009 Published by Elsevier B.V.

1. Introduction

Heterogeneous photocatalysis, a new water and air purification technique, has attracted great attention in the past decade [1,2]. Among many kinds of photocatalysts used up to now, TiO₂ is believed to be a promising photocatalyst for degradation of organic pollutants present in wastewater because of its high activity, low cost, chemical inertness, and photostability [3–5]. However, its photocatalytic activity is still not high enough for practical application. Thus, it is desired to improve photocatalytic activity.

The photocatalytic activity of TiO₂ system mainly depends on its intrinsic properties, such as crystal phase, specific surface area and crystallinity [1,3]. Generally, large surface area is favorable to improve photocatalytic activity. For example, Yu et al. and Alvaro et al. reported mesoporous TiO₂ with large surface area exhibits high photocatalytic activity [6,7]. The large surface area often results from small particle size or porous structure, which usually corresponds to the low anatase crystallinity. The low anatase crys-

tallinity means too many anatase defects, further promoting the recombination of photogenerated electrons and holes [8,9]. Thus, it is expected that increasing anatase crystallinity and retaining large surface area may further improve photocatalytic activity. Recently, our group successfully synthesized high active nanocrystalline TiO₂ photocatalysts by co-modifying with ammonia and cetyltrimethylammonium bromide or by modifying with mesoporous SiO₂, and the enhanced activity was ascribed to high anatase crystallinity and large surface area simultaneously [8,10].

The most popular commercial TiO₂ named by Degussa P25 TiO₂ (P-TiO₂), containing around 85% anatase and 15% rutile, usually exhibits high photocatalytic activity [2,4]. To further improve its photocatalytic activity, several modification attempts have been successfully made. Janus and Morawski reported that the modification of P-TiO₂ was completed under elevated pressure in organic solvent atmosphere, as a result, the carbon modified P-TiO₂ exhibits higher performance for azo dyes decomposition than un-modified one [11]. Yu et al. found that the photocatalytic activity of P-TiO₂ increased after hydrothermal treatment [12]. Yu et al. demonstrated an increase of photocatalytic activity after thermal treatment of P-TiO₂ at 400 °C in air [13]. However, these attempts are all based on increasing hydroxyl groups at the surface of TiO₂. Very recently, many papers reported that phosphate could delay the formation of the anatase phase and inhibit the crystallite growth and the anatase–rutile phase transformation of TiO₂ [14–17]. Our group demonstrated that the phosphorous acid

* Corresponding author at: Key Laboratory of Functional Inorganic Materials Chemistry (Heilongjiang University), Ministry of Education, School of Chemistry and Materials Science, Harbin 150080, P. R. China. Tel.: +86 451 86608616; fax: +86 451 86673647.

** Corresponding author. Tel.: +86 451 86608616; fax: +86 451 86673647.

E-mail addresses: jinglq@hlju.edu.cn (L. Jing), yujief@hit.edu.com (Y. Feng).

modified TiO₂ exhibited higher photocatalytic activity than the unmodified P-TiO₂ [17]. However, few papers about P-TiO₂ modified with phosphorous acid have been reported until now.

In this work, P-TiO₂ has been modified by cheap phosphorous acid for the first time. The phosphorous acid modified Degussa P25 TiO₂ (PP-TiO₂) by thermal treatment at high temperature exhibits higher photocatalytic activity than P-TiO₂. It can be demonstrated that the PO₄³⁻ groups should play important roles in enhancing anatase thermal stability and retaining large surface area, which are responsible for the high photocatalytic activity. This paper would provide a simple strategy to further improve the anatase thermal stability and photocatalytic activity of TiO₂. Expectedly, the enhanced thermal stability of the P-TiO₂ with high activity will expand the application areas of TiO₂, like as coating materials of ceramic tiles with self-cleaning function.

2. Experimental

All used chemicals are of the analytical grade and are used as received without further purification, and doubly deionized water is employed throughout. TiO₂ is Degussa P25 TiO₂.

2.1. Modification of materials

P-TiO₂ is modified by phosphorous acid as the following procedures. Firstly, 1.0 g P-TiO₂ powder is added to a weighing bottle (4 cm × 7 cm) containing 5 mL water under stirring, then continuously stirring for 1 h. Subsequently, 1 mL of phosphorous acid solution (2% mass percentage ratio to TiO₂) is slowly added to the bottle. After ultrasonication for 2 min and stirring for 1 h vigorously, that bottle is kept at 80 °C in the water bath to vaporize the liquid under stirring, then dried at 100 °C for 12 h. Finally, the modified TiO₂ samples are gained by calcining corresponding dried precursors at certain temperature for 2 h, and they are referred to as PP-TiO₂-X, in which X represents the thermal treatment temperature, PP represents the phosphorous acid modified P25 TiO₂. According to the similar procedure mentioned above, the unmodified P25 TiO₂ samples, referred to as P-TiO₂-X, are also obtained.

2.2. Characterization of P-TiO₂

The samples are characterized by X-ray Powder Diffraction (XRD) with a Rigaku D/MAX-rA powder diffractometer (Japan), using Cu K α radiation ($\lambda = 0.15418$ nm), and an accelerating voltage of 30 kV and emission current of 20 mA are employed. The Raman spectra of the samples are recorded with JOBIN YVON HR800 Raman spectrophotometer (France), and the used excitation wavelength is 457.9 nm with an Ar ion laser beam. The specific surface areas of the samples are measured by Brunauer–Emmett–Teller (BET) instrument (Micromeritics automatic surface area analyzer Gemini 2360, Shimadzu), with nitrogen adsorption at 77 K. Transmission Electron Microscopy (TEM) observations are carried out on a JEOL 1200EX operated at an accelerating voltage of 100 kV. The Fourier Transform Infrared Spectra (FT-IR) of the samples are collected with a Bruker Equinox 55 Spectrometer, using KBr as diluents. The surface composition and elemental chemical state of the samples are examined by X-ray Photoelectron Spectroscopy (XPS) using a Model VG ESCALAB apparatus with Mg K α X-ray source, and the binding energies are calibrated with respect to the signal for adventitious carbon (binding energy = 284.6 eV). The Ultraviolet–Visible Diffuse Reflectance Spectra (UV–vis DRS) of the samples are recorded with a Model Shimadzu UV2550 spectrophotometer. The Surface Photovoltage Spectroscopy (SPS) measurements of the samples are carried out with a home-built apparatus that had been described in detail elsewhere [18–20], the powder samples are sandwiched between two ITO glass electrodes,

and the change of surface potential barrier between in the presence of light and in the dark is SPS signal. The raw SPS data are normalized with a Model Zolix UOM-1S illuminometer made in China.

2.3. Evaluation of photocatalytic activity of materials

Rhodamine B (RhB) is one of the common chemicals used widely in the industrial production, which often causes environmental pollution [5]. Therefore, it is chosen as representative organic substance to evaluate the photocatalytic activity of the synthesized TiO₂ samples, and the high photocatalytic degradation rate corresponds to the high photocatalytic activity. The photocatalytic experiments are carried out in a 100 mL of photochemical glass reactor, and the light is provided from a side of the reactor by a 150 W GYZ220 high-pressure Xenon lamp made in China without any filter, which is placed at about 13 cm from the reactor. To examine the photocatalytic degradation rate of RhB, 0.1 g of the TiO₂ sample and 40 mL of 10 mg/L RhB solution are mixed by magnetic stirrer for 30 min in the dark firstly, in order to make the reactive system uniform and the adsorption–desorption equilibrium, then begin to illuminate. After photocatalytic reaction for 1 h, the RhB concentration is analyzed by the optical characteristic absorption at the wavelength of 553 nm of RhB solution after centrifugation with a Model Shimadzu UV2550 spectrophotometer [5]. To obtain the evolution curves of photocatalytic degradation of RhB, 0.2 g of the TiO₂ sample and 80 mL of 20 mg/L RhB solution are employed and the RhB concentrations after photocatalytic reaction for different time are measured.

3. Results and discussion

3.1. Measurements of XRD and Raman

The XRD peaks at $2\theta = 25.28^\circ$ and $2\theta = 27.40^\circ$ are often taken as the characteristic peaks of anatase (1 0 1) and rutile (1 1 0) crystal phase, respectively [20,21]. The mass percentage of anatase phase in the TiO₂ samples can be estimated from the respective integrated characteristic XRD peak intensities using the quality factor ratio of anatase to rutile (1.265), and the crystallite size can also be determined from the broadening of corresponding X-ray spectral peak by Scherrer formula [21]. It can be confirmed from Fig. 1A that the P-TiO₂ has a mixed phase with 85% anatase and 15% rutile, and its anatase crystallite size is about 20 nm. As the thermal treatment temperature rises, the rutile content gradually increases. When the temperature increases to 800 °C, the rutile phase content is nearly 50%. After the thermal treatment at 900 °C, there is only rutile phase. Compared with the P-TiO₂, PP-TiO₂ exhibits high anatase thermal stability since the phase transformation begins to occur at about 800 °C (Fig. 1B), even still with a main anatase phase (75%) after the thermal treatment at 900 °C, demonstrating that the modification with phosphorous acid can effectively inhibit the phase change so as to enhance anatase thermal stability. This is in good agreement with the literature [14–16].

In the Raman spectrum of TiO₂, the peaks, centering at 143, 199, 396, 514 and 636 cm⁻¹, are attributed to the anatase phase, while other peaks, located at 235, 443, 608 and 826 cm⁻¹, are characteristic of the rutile phase [22,23]. It can be confirmed from Fig. 2A that P-TiO₂ contains only anatase phase, which is due to too low amount of rutile phase. However, a small amount of rutile appears in the P-TiO₂-800, and there is only rutile phase in the P-TiO₂-900. Compared with P-TiO₂, PP-TiO₂ has high thermal stability of anatase phase, since the characteristic rutile Raman peaks with rather low intensity can be seen only after the thermal treatment at 900 °C (Fig. 2B).

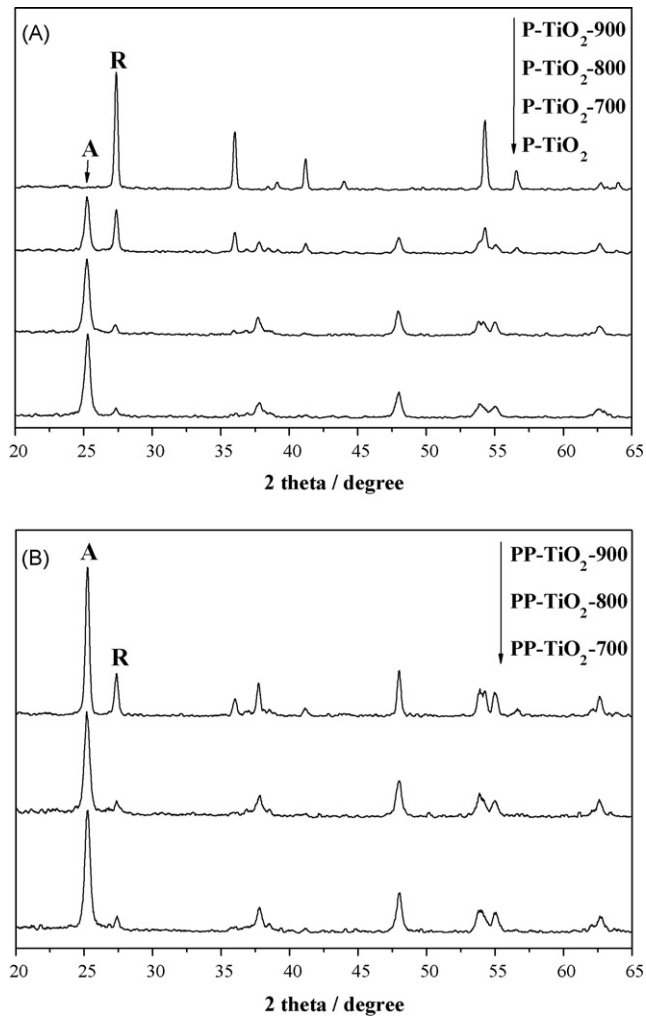


Fig. 1. XRD patterns of different TiO₂.

3.2. Measurements of BET and TEM

P-TiO₂ has a 58.5 m² g⁻¹ BET surface area, as shown in Fig. 3. As the thermal treatment temperature increases, the surface area obviously decreases, and the P-TiO₂-900 has the surface area as small as about 4.3 m² g⁻¹. The small surface area is closely related to the occurrence of a certain amount of rutile phase based on the XRD and Raman results. However, compared with the P-TiO₂, PP-TiO₂ samples have much large surface area at the same thermal treatment temperature.

The TEM photographs of P-TiO₂ (A) and PP-TiO₂-800 (B) are shown in Fig. 4, demonstrating that the two samples have similar morphologies. The P-TiO₂ has about 20 nm average particle size with narrow size distribution (Fig. 4A), indicating that the P-TiO₂ nanocrystals are easily separated. Surprisingly, it can be seen that the particle size of the PP-TiO₂-800 sample nearly does not change a little from Fig. 4B, implying that the modification effectively inhibits the growth of the P-TiO₂ particle. This would be beneficial to still keep large surface area of the PP-TiO₂ by thermal treatment at high temperature.

3.3. Measurements of IR and XPS

To further understand the effects of the modification with the phosphorous acid on the anatase thermal stability and crystallite growth of P-TiO₂, the measurements of IR and XPS were performed.

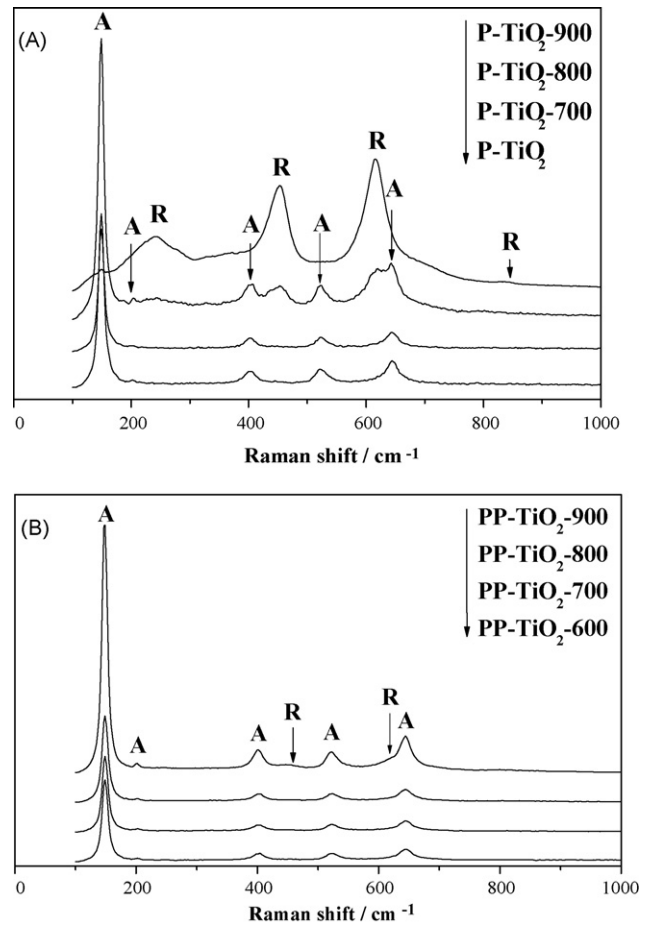


Fig. 2. Raman spectra of different TiO₂.

Fig. 5 shows the FT-IR spectra of different TiO₂ samples. The IR peaks at about 1625 and 3400 cm⁻¹ are ascribed to surface hydroxyl and adsorbed water molecules, respectively [24,25]. As the thermal treatment temperature increases, the 1625 cm⁻¹ peaks of the un-modified and modified samples both gradually decrease, however, PP-TiO₂-700 and PP-TiO₂-800 samples still have more surface hydroxyl and adsorbed water molecules than P-TiO₂. The IR band at 400–850 cm⁻¹ corresponds to the Ti–O–Ti stretching vibration mode in crystal TiO₂ [24,26]. With increasing calcination temper-

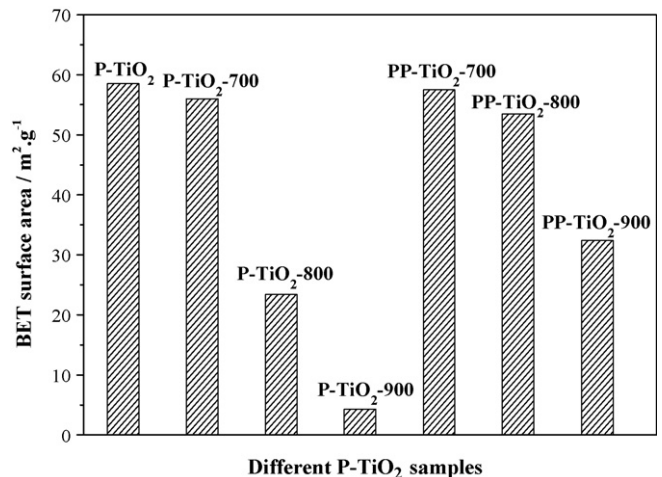


Fig. 3. BET surface area of different TiO₂.

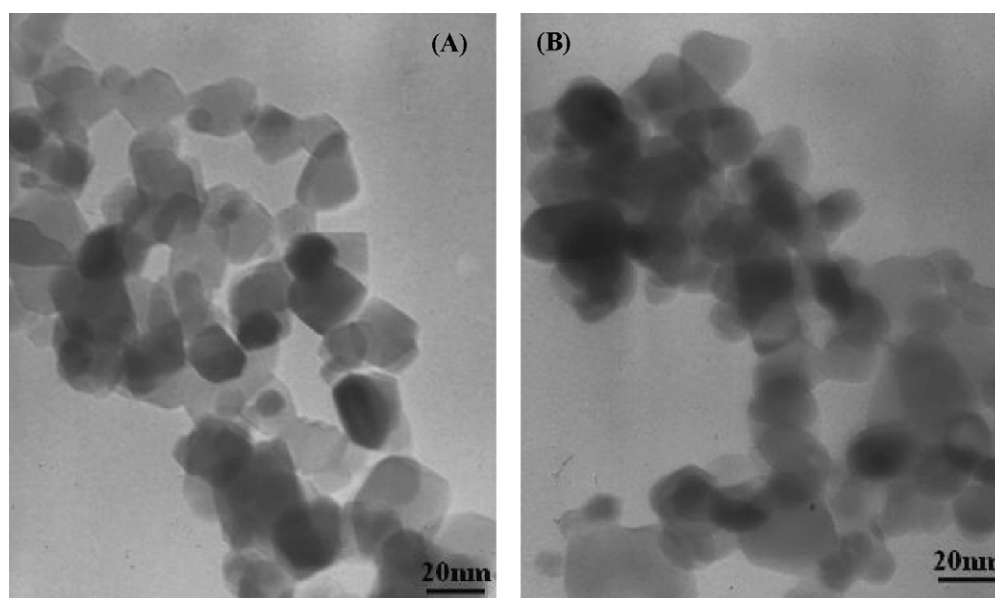


Fig. 4. TEM photographs of (A) P-TiO₂ and (B) PP-TiO₂-800.

ature, the intensity of IR band related to Ti–O–Ti vibration mode also increases. These changes indicate that the corresponding TiO₂ crystallinity becomes high. It should be noticed that, compared with P-TiO₂, all PP-TiO₂ have a new broad IR band at 1010–1250 cm⁻¹, which results from the PO₄³⁻ groups [14,16], demonstrating that the PO₄³⁻ groups added exhibit high thermal stability. Fig. 6 shows XPS spectra of Ti2p (A), O1s (B) and P2p (C) of different TiO₂ samples. The strong Ti2p_{3/2} XPS peaks are all located at about 458.1 eV (Fig. 6A), indicating that the chemical valence of Ti is +4, demonstrating that Ti⁴⁺ is in octahedral coordination with oxygen, other than in tetrahedral environments related to P elements [6,20,27]. The O1s XPS spectra are wide and asymmetric, demonstrating that there are at least two kinds of O chemical states according to the binding energy range from 528.0 to 533.0 eV, including crystal lattice oxygen (O_L) and hydroxyl oxygen (O_H) with increasing binding energy [20,27]. The O_L signal is attributed to the contribution of Ti–O in TiO₂ crystal lattice, and its peak position is at about 529.1 eV. The O_H signal is closely related to the hydroxyl groups resulting mainly from the chemisorbed water, and its peak position is at about 531.8 eV [27]. The weak XPS signals related to O_H

in the PP-TiO₂-700 and PP-TiO₂-800 samples are higher than P-TiO₂, which accords with the small IR peak attributed to surface hydroxyl. According to Fig. 6C, it can be found that the binding energy of P2p is 133.6 eV [6,14], which is characteristic of P element in the phosphorous acid bases, which is in good agreement with IR result.

Since the rutile phase starts to occur at the interfaces between the anatase particles in the agglomerated TiO₂ particles, indicating that the phase transformation usually leads to the remarkable increase in the particle size [28], it can be expected that the phase transformation processes would be suppressed by keeping anatase particles from direct contacts. On the basis of the above consideration and the measurements of IR and XPS, it can be deduced naturally that the PO₄³⁻ groups can effectively hold back the direct contacts between P-TiO₂ nanoparticles by steadily connecting with Ti⁴⁺. However, it should be pointed that the P-TiO₂ sample contained 15% rutile. Therefore, it is suggested that, besides keeping from the directing connections between P-TiO₂ nanoparticles, the inhibition effects of the PO₄³⁻ groups on the surface mass diffusion of P-TiO₂ should also be considered much. In addition, the expected great decrease in the surface energy, which results from the modification with phosphorous acid bases, is beneficial to suppress the phase change.

To further reveal the modification mechanisms of phosphorous acid on P-TiO₂, similar experiments are also carried out by modifying with other acids, such as hydrochloric acid, acetic acid and nitric acid, in place of phosphorous acid, respectively. The XRD results show that the modification with the other three acids cannot nearly enhance the anatase thermal stability of P-TiO₂, even with a little promotion effect (see supporting information (SI)-1), which is attributed to the weak thermal stability of the used three acids and their weak interactions with TiO₂. These similar experiments strongly support that the PO₄³⁻ groups with high thermal stability should play important roles in the inhibition of phase change and crystallite growth of P-TiO₂.

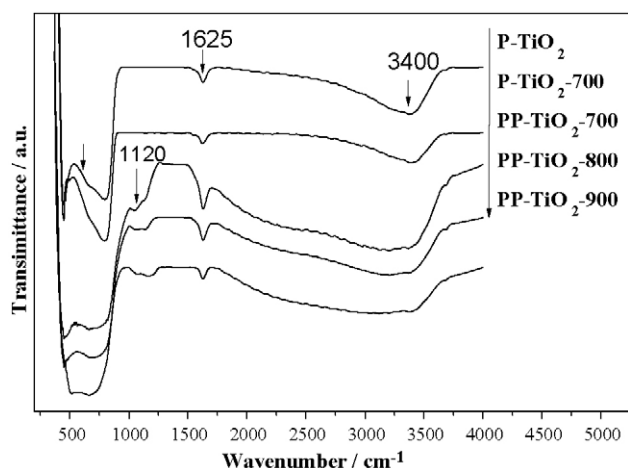


Fig. 5. FT-IR spectra of different TiO₂.

3.4. Measurements of UV–vis DRS and SPS

The UV–vis DRS spectra of P-TiO₂, P-TiO₂-800 and PP-TiO₂-800 samples are shown in Fig. 7. Compared with P-TiO₂, the DRS

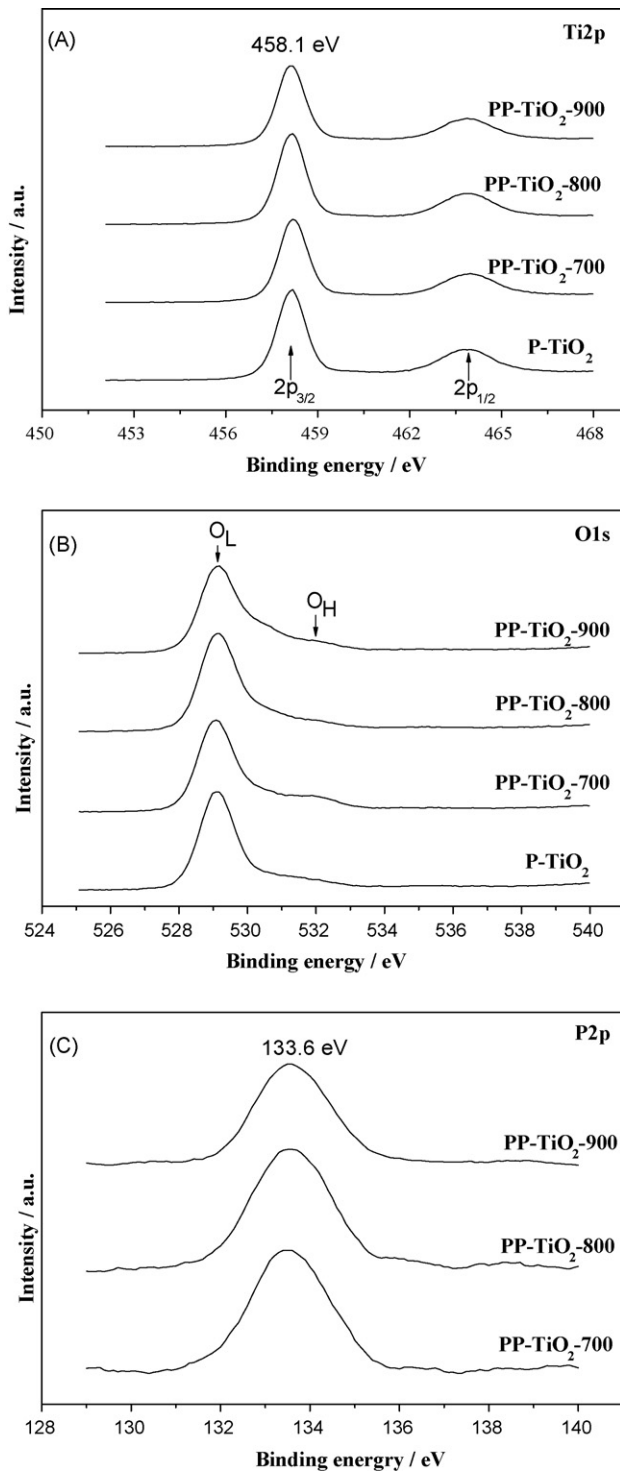


Fig. 6. XPS spectra of different TiO_2 .

of P- TiO_2 -800 exhibits a marked red-shift, which is ascribed to the rutile formation and the crystallite growth. However, the DRS of PP- TiO_2 -800 sample does not change a little nearly, indicating that its crystal phase composition and corresponding crystallite size retain unchanged. This is in accordance with XRD and TEM results.

On the basis of the SPS principle [18,19], it can be expected that the stronger is the SPS response, the higher is the photoinduced charge carriers. The SPS responses of different TiO_2 samples are shown in Fig. 8. It can be noticed that the SPS response of PP- TiO_2

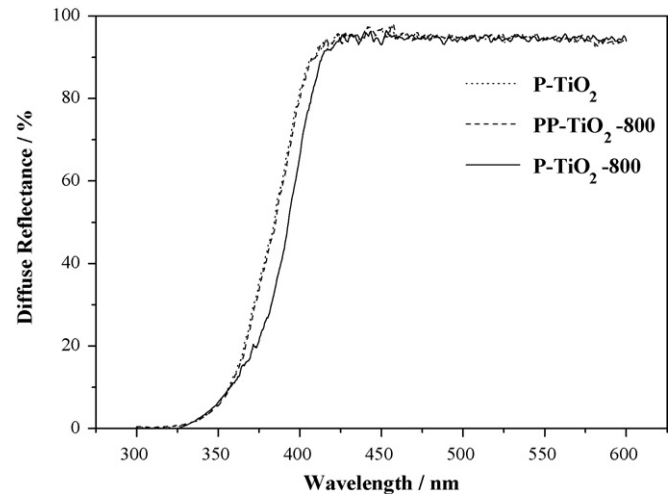


Fig. 7. DRS spectra of different TiO_2 .

gradually becomes strong with increasing the treatment temperature. The high treatment temperature enhances the anatase crystallinity of TiO_2 , especially for surface phase, on the condition of keeping unchanged, further making the electronic band structure perfect and the defect amount decreasing. As a result, the photoinduced charge separation is improved. However, the PP- TiO_2 -900 has a weak SPS response, which is due to too much of rutile phase. Noticeably, compared with P- TiO_2 , all the PP- TiO_2 samples, even by thermal treatment at high temperature, display low SPS responses, which mainly results from the PO_4^{3-} groups on the surfaces of PP- TiO_2 .

3.5. Evaluation of photocatalytic activity

The RhB photocatalytic degradation rates, which equal to the differences between the total degradation and the adsorption degradation, on the different TiO_2 samples, are shown in Fig. 9A. Compared with the photocatalytic degradation, so small amount (about 1%) of direct photolysis rate of RhB is neglectable. To further confirm the activity orders of different TiO_2 samples, the evolution curves of photocatalytic degradation of the RhB on the several TiO_2 samples are shown in Fig. 9B. It can be seen in Fig. 9A, as the thermal treatment temperature increases, the photocatalytic activity of the P- TiO_2 -X samples gradually decreases, which is attributed to the rutile content increase and then the surface area decrease. Interestingly, the PP- TiO_2 -X samples exhibit much higher photo-

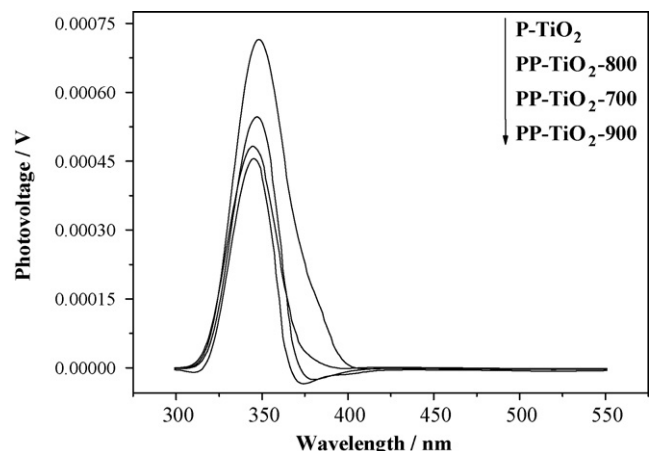


Fig. 8. SPS responses of different TiO_2 .

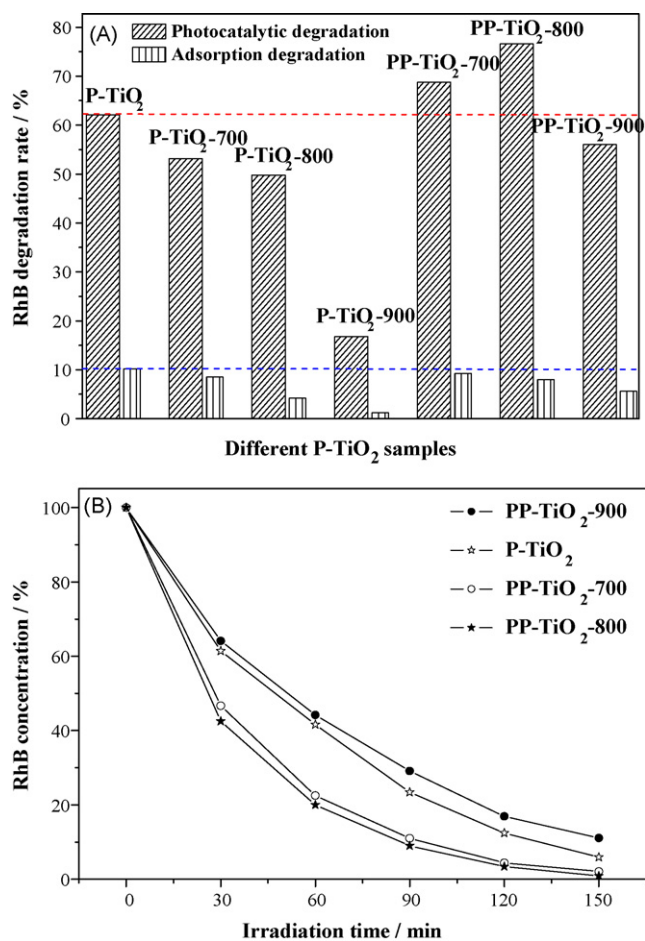


Fig. 9. Photocatalytic degradation rates (A) and photocatalytic degradation evolution curves (B) of RhB solution on the different TiO₂ samples.

catalytic activity than P-TiO₂-X samples at the same treatment temperature, especially for the PP-TiO₂-700 and PP-TiO₂-800 two samples superior to the P-TiO₂ sample. However, all the other three acids modified P-TiO₂ samples by thermal treatment at high temperature have lower photocatalytic activity than the P-TiO₂ (see SI-II), demonstrating that the modification with phosphorous acid has obviously different effects on the P-TiO₂ compared with the modifications of other acids. Moreover, the selected samples in Fig. 9B exhibit the same activity orders as in Fig. 9A, and after photocatalytic reaction for 150 min, the RhB degradations over the PP-TiO₂-700 and PP-TiO₂-800 two samples reach 100% nearly.

On the basis of the above characterization results, combining with the photocatalytic degradation data of RhB, the activity enhancement mechanisms can be suggested, which mainly is involved with high photoinduced charge separation rate and still large surface area. The increase in the charge separation rate is closely related to the enhancement in the anatase thermal stability. Meanwhile, the large surface area is kept, which is favorable for catalytic reactions. For example, after thermal treatment at 800 °C, the PP-TiO₂-800 has a slight decrease by 3 m² g⁻¹ in the surface area compared with P-TiO₂. Thus, it can be deduced that the combination of the high photoinduced charge separate rate and large surface area is responsible for the high photocatalytic activity of the PP-TiO₂-800. Moreover, a certain amount of surface hydroxyl also favors photocatalytic degradations. As expected, the PP-TiO₂-900 displays low photocatalytic activity, which is due to too much of rutile and small surface area.

4. Conclusions

P-TiO₂ has been successfully modified by the post-treatment with the phosphorous acid. The modification with phosphorous acid effectively enhances the anatase thermal stability and then keep large surface area simultaneously, which mainly results from the inhibition effects of the PO₄³⁻ groups on the surface mass diffusion and the aggregations among P-TiO₂ particles during the thermal treatment. The enhanced anatase thermal stability is beneficial to promote photoinduced charge separation. The high charge separation rate and large surface area, altogether with a certain amount of surface hydroxyls, lead to the high photocatalytic activity of the PP-TiO₂-800 for degrading RhB solution, even superior to the P-TiO₂. It can be suggested that the final photocatalytic performance mainly depends on the combination effects of the photoinduced charge separation situation and the surface area. This work further provides new physical insights on the phase transformation of TiO₂, and an effective modification approach of nanosized TiO₂ for excellent photocatalytic performance.

Acknowledgements

This work is financially supported from the National Nature Science Foundation of China (No. 20501007), the Programme for New Century Excellent Talents in Universities (NCET-07-0259), the Key Project of Science & Technology Research of Ministry of Education of China (No. 207027), the Science Foundation of Excellent Youth of Heilongjiang Province of China (JC200701), and State Key Lab of Urban Water Resource and Environment (HIT) (QAK200803).

Appendix A. Supplementary data

Supplementary data associated with this article can be found, in the online version, at doi:10.1016/j.jhazmat.2009.07.120.

References

- [1] M.R. Hoffmann, S.T. Martin, W. Choi, D.W. Bahnemann, Environmental applications of semiconductor photocatalysis, *Chem. Rev.* 95 (1995) 69–96.
- [2] M.I. Litter, Heterogeneous photocatalysis: transition metal ions in photocatalytic systems, *Appl. Catal. B* 23 (1999) 89–114.
- [3] M.A. Fox, M.T. Dulay, Heterogeneous photocatalysis, *Chem. Rev.* 93 (1993) 341–357.
- [4] A. Hagfeldt, M. Gratzel, Light-induced redox reactions in nanocrystalline systems, *Chem. Rev.* 95 (1995) 49–68.
- [5] J.C. Zhao, T.X. Wu, K.Q. Wu, K. Oikawa, H. Hidaka, N. Serpone, Photoassisted degradation of dye pollutants. 3. Degradation of the cationic dye Rhodamine B in aqueous anionic surfactant/TiO₂ dispersions under visible light irradiation: evidence for the need of substrate adsorption on TiO₂ particles, *Environ. Sci. Technol.* 32 (1998) 2394–2400.
- [6] J.C. Yu, L.Z. Zhang, Z. Zheng, J.C. Zhao, Synthesis and characterization of phosphated mesoporous titanium dioxide with high photocatalytic activity, *Chem. Mater.* 15 (2003) 2280–2286.
- [7] M. Alvaro, C. Aprile, M. Benitez, E. Carbonell, H. Garcia, Photocatalytic activity of structured mesoporous TiO₂ materials, *J. Phys. Chem. B* 110 (2006) 6661–6665.
- [8] G.H. Tian, H.G. Fu, L.Q. Jing, B.F. Xin, K. Pan, Preparation and characterization of stable biphasic TiO₂ photocatalyst with high crystallinity, large surface area, and enhanced photoactivity, *J. Phys. Chem. C* 112 (2008) 3083–3089.
- [9] S.C. Pillai, P. Periyat, H. George, D.E. McCormack, M.K. Seery, H. Hayden, J. Colreavy, D. Corr, S.J. Hinder, Synthesis of high-temperature stable anatase TiO₂ photocatalyst, *J. Phys. Chem. C* 111 (2007) 1605–1611.
- [10] C.H. Kang, L.Q. Jing, T. Guo, H.C. Cui, J. Zhou, H.G. Fu, Mesoporous SiO₂-modified nanocrystalline TiO₂ with high anatase thermal stability and large surface area as efficient photocatalyst, *J. Phys. Chem. C* 113 (2009) 1006–1013.
- [11] M. Janus, A.W. Morawski, New method of improving photocatalytic activity of commercial Degussa P25 for azo dyes decomposition, *Appl. Catal. B* 75 (2007) 118–123.
- [12] J.G. Yu, H.G. Yu, B. Cheng, M.H. Zhou, X.J. Zhao, Enhanced photocatalytic activity of TiO₂ powder (P25) by hydrothermal treatment, *J. Mol. Catal. A* 253 (2006) 112–118.
- [13] J.C. Yu, J. Lin, D. Lo, S.K. Lam, Influence of thermal treatment on the adsorption of oxygen and photocatalytic activity of TiO₂, *Langmuir* 16 (2000) 7304–7308.

- [14] L. Korosi, S. Papp, I. Bertoti, I. Dekany, Surface and bulk composition, structure, and photocatalytic activity of phosphate-modified TiO₂, *Chem. Mater.* 19 (2007) 4811–4819.
- [15] L. Lin, R.Y. Zheng, J.L. Xie, Y.X. Zhu, Y.C. Xie, Synthesis and characterization of phosphor and nitrogen co-doped titania, *Appl. Catal. B* 76 (2007) 196–202.
- [16] L. Korosi, A. Oszko, G. Galbacs, A. Richardt, V. Zollmer, I. Dekany, Structural properties and photocatalytic behaviour of phosphate-modified nanocrystalline titania films, *Appl. Catal. B* 77 (2007) 175–183.
- [17] X. Qin, L.Q. Jing, L.P. Xue, Y.B. Luan, H.G. Fu, Phosphorous acid modified TiO₂ nanoparticle photocatalysts, *Chin. J. Inorg. Chem.* 24 (2008) 1108–1112.
- [18] L.Q. Jing, Z.L. Xu, J. Shang, X.J. Sun, W.M. Cai, H.G. Fu, Review of surface photovoltage spectra of nano-sized semiconductor and its applications in heterogeneous photocatalysis, *Sol. Energy Mater. Sol. C* 79 (2003) 133–151.
- [19] Y.H. Lin, D.J. Wang, Q.D. Zhao, M. Yang, Q.L. Zhang, A study of quantum confinement properties of photogenerated charges in ZnO nanoparticles by surface photovoltage spectroscopy, *J. Phys. Chem. B* 108 (2004) 3202–3206.
- [20] L.Q. Jing, B.F. Xin, F.L. Yuan, Effects of surface oxygen vacancies on photophysical and photochemical processes of Zn-doped TiO₂ nanoparticles and their relationships, *J. Phys. Chem. B* 110 (2006) 17860–17865.
- [21] Q.H. Zhang, L. Gao, J.K. Guo, Effects of calcination on the photocatalytic properties of nanosized TiO₂ powders prepared by TiCl₄ hydrolysis, *Appl. Catal. B* 26 (2000) 207–215.
- [22] T. Ohsaka, F. Izumi, Y. Fujiki, Raman spectrum of anatase, TiO₂, *J. Raman Spectrosc.* 7 (1978) 321–324.
- [23] C.C. Hyun, M.J. Young, B.K. Seung, Size effects in the Raman spectra of TiO₂ nanoparticles, *Vib. Spectrosc.* 37 (2005) 33–38.
- [24] L.Q. Jing, H.G. Fu, B.Q. Wang, D.J. Wang, B.F. Xin, S.D. Li, J.Z. Sun, Effects of Sn dopant on the photoinduced charge property and photocatalytic activity of TiO₂ nanoparticles, *Appl. Catal. B* 62 (2006) 282–291.
- [25] Z. Ding, G.Q. Lu, P.F. Greenfield, Role of the crystallite phase of TiO₂ in heterogeneous photocatalysis for phenol oxidation in water, *J. Phys. Chem. B* 104 (2000) 4815–4820.
- [26] V.N. Sigaev, P. Pernice, A. Aronne, O.V. Akimova, S.Y. Stefanovich, A. Scaglione, Surface studies of TiO₂–SiO₂ glasses by X-ray photoelectron spectroscopy, *J. Non-Cryst. Solids* 126 (1990) 202–208.
- [27] J.G. Yu, H.G. Yu, B. Cheng, X.J. Zhao, J.C. Yu, W.K. Ho, The effect of calcination temperature on the surface microstructure and photocatalytic activity of TiO₂ thin films prepared by liquid phase deposition, *J. Phys. Chem. B* 107 (2003) 13871–13879.
- [28] J. Zhang, M.J. Li, Z.C. Feng, J. Chen, C. Li, UV Raman spectroscopic study on TiO₂. I. Phase transformation at the surface and in the bulk, *J. Phys. Chem. B* 110 (2006) 927–935.